Quasistationary structures on a class of forced Burgers turbulence between walls

Hiroshi Nakazawa
Department of Physics, Kyoto University, Kyoto 606, Japan
(Received 27 October 1986)

The temporally stationary state of Burgers fluid between walls is discussed in the inviscid limit under a class of external, random forcing. The force and the fixed boundaries are shown to pose determinate restrictions on the fluid motion in the large, and drive the Burgers fluid to construct, and to alternate between, a few characteristic structures for dissipation. A mean-field approximation is presented with its inviscid-limit closed solutions for average profiles in the stationary state. The solutions are not unique and reproduce, though with varying accuracies, the mentioned structures of the fluid motion. Results of numerical runs are also reported, and their statistics is shown to admit reconstructions on this picture, confirming further the existence of these quasistationary structures and the itinerant motion of the fluid among them.

I. INTRODUCTION

We discuss the motion of Burgers fluid[1] between walls with small viscosity coefficient ν. The fluid is supposed to undergo random excitations due to a simple class of external mechanisms. The aim of this work is in the temporally stationary, stochastic motion of the fluid. The basic equation takes the form

$$\partial u_\nu(x,t)/\partial t+\tfrac{1}{2}\partial u_\nu^2/\partial x=\nu\partial^2 u_\nu/\partial x^2+\sigma(x)f(t)\ , \qquad x\in X\equiv[0,\pi] \quad (1)$$

$$u_\nu(x,t)\,|_{\partial X}=\sigma(x)\,|_{\partial X}=0\ , \qquad u_\nu(x,s)=\psi(x)\ \text{given},\quad \nu>0 \quad (2)$$

with $|_{\partial X}$ for values at the boundary of X.[2] The nonrandom function $\sigma(x)$ represents specifically a large-scale Fourier mode such as $(2/\pi)^{1/2}\sin x$, and is assumed to satisfy the normalization condition

$$\int_X \sigma^2(x)dx=1\ . \quad (3)$$

$f(t)$ is always taken to be a Gaussian white noise with expectations

$$\langle f(t)\rangle=0,\quad \langle f(t)f(t+\tau)\rangle=\delta(\tau)\ . \quad (4)$$

Equations (1)–(4) arise as a normalized, central-limit form[3] of a class of forced Burgers turbulence problems, and stipulate that the energy $E(t)=\frac{1}{2}\int_X u_\nu^2(x,t)dx$ of $u_\nu(x,t)$ undergoes random injection at the average rate $\frac{1}{2}$. For Eq. (1) with possibly more general forms of its force term $\sigma(x)f(t)$, several ruling conclusions are known[4,5] on (especially x- and t-local) behaviors for $\nu\downarrow 0$ of $u_\nu(x,t)$. If $\sigma''(x)$ is Hölder continuous, the solution $u_\nu(x,t)$ for any initial data $\psi(x)\in L^\infty(X)$ is twice differentiable in x and converges samplewise as $\nu\downarrow 0$ in the space $L^1(X)$ of functions of x, $\forall t>s$. In particular, if $\nu>0$ but small, there can arise on a sample of $u_\nu(x,t)$ steep downward steps in a range $|x-S(t)|\leqq O(\nu)$ around $S(t)$ (say) with the form

$$u_\nu(x,t)\cong S'(t)-\tfrac{1}{2}D(t)\tanh\{D(t)[x-S(t)]/4\nu\}\ . \quad (5)$$

This represents the *sole* possible form of balance of terms of $O(1/\nu)$ in (1) for $\nu\sim+0$, $\frac{1}{2}\partial\bar{u}_\nu^2/\partial\bar{x}=\nu\partial^2\bar{u}_\nu/\partial\bar{x}^2$ with $\bar{u}_\nu\equiv u_\nu-S'(t)$ and $\bar{x}\equiv x-S(t)$. Consequently, any $\psi(x)\in L^\infty(X)$ gives for $\forall t>s$ sample functions of $u(x,t)\equiv u_{+0}(x,t)$, the suitable representative of the $L^1(X)$ limit for $\nu\downarrow 0$ of $u_\nu(x,t)$, that have bounded variations in x; they satisfy the entropy condition[6,5] $u(x-0,t)\geqq u(x+0,t)$, $\forall x\in X$, and can have shock discontinuities [as before at $x=S(t)$, say] that move according to

$$dS(t)/dt=\tfrac{1}{2}[u(S(t)-0,t)+u(S(t)+0,t)]\ . \quad (6)$$

If $\sigma(x)$ and $\psi(x)$ are regular functions of $x\in X$, $u(x,t)$ is further restricted to having samples consisting of finite numbers of shock discontinuities and interpolating regular segments[5] with probability 1, $\forall t>s$. Thus the small scale (hence large wave-number) structures of the forced field $u_\nu(x,t)$ for $\nu\geqq+0$ are known to some extent of universality, if only $\sigma(x)$ has a sufficient degree of smoothness.

In comparison, our sights have remained dark on the temporally stationary states to be established on $u_\nu(x,t)$ as $s\downarrow-\infty$. It has not been known what types of large-scale structures arise on samples of $u(x,t)$, not to mention typical values associated with average profiles. As a matter of course, numerical simulations of (1) were performed[7] for ν small but positive as described fully in Sec. V, taking advantage of the known $L^1(X)$ convergence for $\nu\downarrow 0$. Runs revealed very simple behaviors of $u_\nu(x,t)$, which were partly anticipated theoretically,[8] but still surprised us in various respects. For the case of $\sigma(x)=(2/\pi)^{1/2}\sin x$, the tendency may be summarized as follows: A sample of $u_\nu(x,t)$ for ν small invariably takes a smooth profile, increasing to the right without recognizable wiggling or shock fronts on its central portion; it shows erratic motions which are centered around three typical profiles depicted in Fig. 1 keeping the mentioned simple forms; there are occasional transitions among these groups of profiles to which unexceptionally correspond signs of the total momentum $P(t)\equiv\int_X u_\nu(x,t)dx$.

The theme of the present work is this behavior of (1) which we would like to comprehend analytically as a pos-

sible facet of turbulence phenomena. The work will show the following.

[1] There exist some basic restrictions, imposed on the large-scale structures and their time-local kinematics of $u_\nu(x,t)$ for small $\nu>0$, that arise from the presence of walls and the force. These restrictions in particular drive zeros on a profile of $u_\nu(x,t)$ to a few, nearly fixed points, and force the velocity field to construct some large-scale structures for dissipation around profiles of Fig. 1.

[2] However, these respective structures in isolation cannot form stationary states. The stationary state of $u_\nu(x,t)$ for $\nu \geqq +0$ should be unique, suggesting that it will be constructed as random itinerations stated above, from one of these structures to others.

[3] A mean-field approximation of (1), to be called a model, exists with its closed solutions for the stationary state in the inviscid limit. The solutions are not unique, reproducing separately the global structures described in [1] though with varying degrees of accuracy.

[4] The model closed solutions and some further devices construct a statistics on the picture of [2], reproducing the tendency of numerically obtained moments of $u_\nu(x,t)$ up to the fourth degree. This [4] would give a conclusive, analytical evidence for the existence of the structures on (1) as stated in [2].

Section II gives analyses on some local and global structures of sample fields of (1) from viewpoints pertinent to (2)—(4). Section III introduces the model. Its solutions are described in Sec. IV A, and the reconstruction of the statistics of u_ν is presented in Sec. IV B. Section V exposes the details of numerical simulations of (1). Concluding remarks will follow in Sec. VI.

II. LOCAL AND GLOBAL STRUCTURES

We discuss some analytical implications of (1) that are pertinent to local and global structures of $u_\nu(x,t)$ proper to the existence of forces and fixed boundaries. If no other inference is made, we take such $\sigma(x)$ that has no zero on $0<x<\pi$ with a sufficient regularity.

A. Momentum and energy dissipation

If $\nu>0$, (1) and (2) give the following for the total momentum $P(t)$ of the fluid at $\forall t>s$ for $\forall\psi(x)\in L^\infty(X)$:

$$dP/dt=\nu\frac{\partial u_\nu(x,t)}{\partial x}\Big|_{x=0}^{x=\pi}+\Sigma f(t)\ ,\qquad \Sigma\equiv\int_X\sigma(x)dx\ . \tag{7}$$

By the assumed $\Sigma\neq 0$, $\Sigma f(t)$ in (7) gives a divergent behavior $\propto\Sigma(t-s)^{1/2}$ for $P(t)\sim\Sigma B(t)$ with the Wiener process $B(t)=\int_s^t f(r)dr$. This tendency is opposed by the first term on the right-hand side, which persists even in the limit $\nu\downarrow 0$.[9] In order to explain this with the explicit form of the limit, we assume regular $\sigma(x)$ and $\psi(x)$. Let $(S_0\equiv 0<)S_1(t)<\cdots<S_n(t)(<S_{n+1}\equiv\pi)$ be shock fronts on a sample of $u(x,t)\equiv u_{+0}(x,t)$. We have

$$\begin{aligned}dP/dt=\sum_{k=0}^{n}\Big[&-\tfrac{1}{2}u^2(x,t)\Big|_{S_k(t)}^{S_{k+1}(t)}\\&+u(S_{k+1}(t)-0,t)S'_{k+1}(t)\\&-u(S_k(t)+0,t)S'_k(t)\Big]+\Sigma f(t)\ .\end{aligned}$$

The Rankine-Hugoniot relation (6) gives the desired inviscid-limit form,

$$dP/dt=\tfrac{1}{2}u^2(+0,t)-\tfrac{1}{2}u^2(\pi-0,t)+\Sigma f(t),\quad \nu=+0\ . \tag{8}$$

Since walls $x=0$ and $x=\pi$ can have only stationary shock discontinuities with $S'(t)=0$, $u(+0,t)\leqq 0$ and $u(\pi-0,t)\geqq 0$ hold by the entropy condition. A portion on the profile with $u(x,t)<0$ (or >0, respectively) is self-convected to the left (or the right). Therefore, terms $\frac{1}{2}u^2(+0,t)$ or $-\frac{1}{2}u^2(\pi-0,t)$ on the right-hand side of (8) represent, respectively, the draining of negative or positive momenta into wall shock discontinuities. Other shock fronts in the fluid conserve the momentum by (6). Thus (8) remains valid for $\forall\psi(x)\in L^\infty(X)$ at $\forall t>s$.

Similarly, the total energy $E(t)$ is also dissipated at $\nu=+0$, now at *all* shock fronts on a profile. We quote[5] the Itô-type form of $E'(t)$ for $\nu=+0$:

$$\begin{aligned}dE(t)/dt=-\tfrac{1}{12}\sum_{k=1}^{n}&[u(S_k(t)-0,t)-u(S_k(t)+0,t)]^3\\&+\tfrac{1}{3}u^3(+0,t)-\tfrac{1}{3}u^3(\pi-0,t)\\&+\tfrac{1}{2}+\int_X u(x,t)\sigma(x)dx\,f(t)\ .\end{aligned} \tag{9}$$

B. Motion of zeros on regular segments

Let $Z(t)$ denote a zero on a regular segment[3] of $u(x,t)$. We need the tendency of the motion of $Z(t)$. To this end we denote $u'_\nu(x,t)\equiv\partial u_\nu(x,t)/\partial x$ and $u''_\nu\equiv\partial^2 u_\nu/\partial x^2$, and state the following.

Given a profile $u_\nu(x,t)$ of (1) with $\nu>0$ for regular $\sigma(x)$ and $\psi(x)$, the conditional average velocity

$$\langle dZ(t)/dt\rangle_c\equiv\langle Z'(t)\rangle_c$$

of $Z(t)$, defined by $u_\nu(Z(t),t)=0$ together with the restriction $u'_\nu[Z(t),t]>0$, has the following expression:

$$\begin{aligned}&\langle Z'(t)\rangle_c=F(Z(t),t)\ ,\\&F(x,t)=-\nu\partial[\ln u'_\nu(x,t)]/\partial x\\&\qquad+[2u'_\nu(x,t)]^{-1}\partial[\sigma^2(x)/u'_\nu(x,t)]/\partial x\ .\end{aligned} \tag{10}$$

Define $v(x,t)\equiv u_\nu(x,t)-\sigma(x)B(t)$, $B(t)\equiv\int_s^t f(r)dr$. This $v(x,t)$ is continuously differentiable, twice in x and

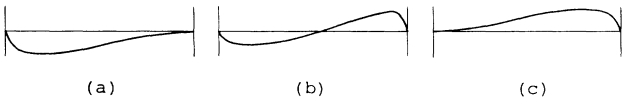

FIG. 1. Schematic profiles of $u_\nu(x,t)$ for (a) $P(t)<0$, (b) $P(t)\sim 0$, and (c) $P(t)>0$ for the case $\sigma(x)\propto\sin x$.

once in t with probability 1, and obeys

$$\partial v/\partial t=\nu\partial^2 u_\nu/\partial x^2-\tfrac{1}{2}\partial u_\nu^2/\partial x \ .$$

There holds $0=v(Z(t),t)+\sigma(Z(t))B(t)$. Assuming the Itô-type stochastic differential $dZ(t)=\sigma(Z(t))B(t)$. Assuming the Itô-type stochastic differential $dZ(t)=\alpha(t)dt+\beta(t)dB(t)$ and applying Itô's formula[10] on $v(Z(t),t)$ and $\sigma(Z(t))\times B(t)$, we have a stochastic differential equation in Itô's sense:

$$dZ(t)/dt=F(Z(t),t)-[\sigma(Z(t))/u'(Z(t),t)]f(t) \ . \qquad (11)$$

The first term on the right-hand side proves (10). Sorry to say, $v(x,t)$ is not a deterministic function, and this application of Itô's formula seems not justified in the strict sense. Therefore, a heuristic derivation of (10) is presented in Appendix A.

On the right-hand side of $F(x,t)$, the first term represents the nonforced case $\sigma(x)\equiv 0$. It vanishes as $\nu\downarrow 0$ for $Z(t)$'s of our concern, though in shock fronts with $u'_\nu(Z(t),t)<0$ it converges to $S'(t)$ of (6) by the equation of $O(1/\nu)$ terms, $\nu u''_\nu\simeq[u_\nu-S'(t)]u'_\nu$. As to the second term of $F(x,t)$, we note that profiles shown in Fig. 1 give similar $u'_\nu(x,t)$'s, putting aside their behaviors near walls. Therefore, this term [hence $F(x,t)$] for $\nu\sim+0$ in (10) depends not much on these conditioning profiles of relevance. Assuming $\sigma(x)=(2/\pi)^{1/2}\sin x$, we depict $F(x,t)$ for $\nu\sim+0$ in Fig. 2, corresponding, respectively, to $u_\nu(x,t)$ of Fig. 1. It should be noted that only portions of these curves drawn in solid lines (not in dotted lines) can exhibit the tendency of $\langle Z'(t)\rangle_c$, because there must hold $u_\nu(Z(t),t)=0$ and $u'_\nu(Z(t),t)>0$ in (10).

The above statement assumed the existence of $Z(t)$ and gave its tendency in motion. As to the way of the birth of such a $Z(t)$, numerical runs reveal a simple circumstance again: Throughout runs which are up to $t\sim 40$ (cf. Sec. V), a new zero on $u_\nu(x,t)$ for small ν was observed to be born only through the process (a)→(d) shown in Fig. 3 or their inversions $u_\nu(x,t)\to -u_\nu(\pi-x,t)$, despite many other conceivable processes. The birth notably occurs only at those x's with $u'_\nu(x,t)\simeq 0$, as shown in Fig. 3(b).[11] We may thus conclude the following. Zeros on $u_\nu(x,t)$ for $\nu\sim+0$, among which we exclude the trivial ones at $x=0$ and $x=\pi$, are at most unique throughout the history, and it tends on the average to three nearly fixed points, one at $x\sim\pi/2$ and others at $x\sim 0$ and π. The attraction to $x\sim 0$ or π is stronger in comparison to $x\sim\pi/2$. These *attractors*, however, are mirages formed by the profile $u_\nu(x,t)$ itself that appear only when $u_\nu(x,t)$ is sustained to some level (i.e., when ν is small[3]) by the energy injection due to the force.

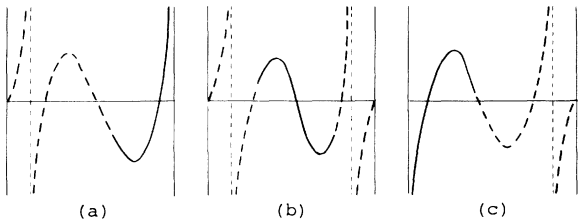

FIG. 2. Schematic graphs of $\langle Z'(t)\rangle_c$ vs $Z(t)\in[0,\pi]$ corresonding to conditioning profiles of Fig. 1 (a)—1(c), respectively.

C. Global estimates and structures

In this subsection we use the notation $u_\nu(x,t;\psi)$ for the solution of (1)—(4). Denote

$$D(x,t)\equiv u_\nu(x,t;\psi)-u_\nu(x,t;\psi^*) \ ,$$

where both u_ν's on the right-hand side refer to the same realization of $f(t)$. By (1) and (2) we have[12] for $\nu>0$

$$\begin{aligned}(d/dt)\int_X \mathrm{sgn}[D(x,t)]D(x,t)dx &= \int_X \mathrm{sgn}[D(x,t)]D_t(x,t)dx \\ &= \nu\int_X \mathrm{sgn}[D(x,t)]D_{xx}(x,t)dx \qquad (12a)\\ &\leqq \nu\{\mathrm{sgn}[D(\pi-0,t)]D_x(\pi,t)-\mathrm{sgn}[D(+0,t)]D_x(0,t)\} \qquad (12b)\\ &\leqq 0 \ . \qquad (12c)\end{aligned}$$

In the transition from (12a) to (12c) we have gradually dropped some of the contributions from points at which $D(x,t)$ changes its sign; such a contribution is seen to be negative by examining possible local profiles of $D(x,t)$. The above (12c) implies $L^1(X)$-contracting character of the motion of $u_\nu(x,t)$ for $\forall\nu\geqq+0$,

$$\int_X |u_\nu(x,t;\psi)-u_\nu(x,t;\psi^*)|\,dx\leqq\int_X|\psi(x)-\psi^*(x)|\,dx \ . \qquad (13)$$

A more detailed form (12b) gives the following information for $\nu\ll 1$:

$$\begin{aligned}(d/dt)\int_X |u_\nu(x,t;\psi)-u_\nu(x,t;\psi^*)|\,dx \leqq & -\tfrac{1}{2}|u^2(+0,t;\psi)-u^2(+0,t;\psi^*)| \\ & -\tfrac{1}{2}|u^2(\pi-0,t;\psi)-u^2(\pi-0,t;\psi^*)|+O(\nu)\leqq 0 \ , \qquad (14)\end{aligned}$$

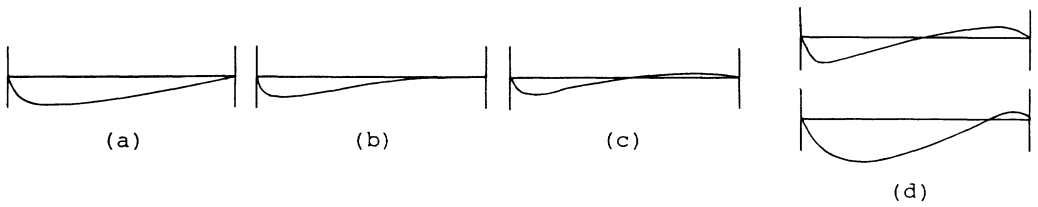

FIG. 3. The process of birth of a new Z for $\sigma(x) \propto \sin x$.

where $u(x,t;\psi)$ stands for $u_{+0}(x,t;\psi)$ and use was made of the following obtained from (5):[13]

$$\nu u_\nu'(\pi,t) = -\tfrac{1}{2}u^2(\pi-0,t)+O(\nu) ,$$

$$u_\nu'(0,t) = -\tfrac{1}{2}u^2(+0,t)+O(\nu) .$$

In view of the effect of self-convection, we may safely assume that any difference $u_\nu(x,t;\psi)-u_\nu(x,t;\psi^*)\neq 0$ will eventually be convected to walls (or to internal centers of antisymmetry[13]). Thus (14) implies

$$\lim_{s\downarrow-\infty}\int_X |\, u_\nu(x,t;\psi)-u_\nu(x,t;\psi^*)\,|\, dx = 0 ,$$

$$\forall \nu \geqq +0, \quad \forall \psi,\psi^* \in L^\infty(X) , \qquad (15)$$

the uniqueness of the stationary state of $u_\nu(x,t)$. Equation (1) poses an ergodic, Ljapunov stable motion in $L^1(X)$; for this stability (13), cf. Sec. VI further. Note also for general $\sigma(x)$ that the inversion $u_\nu(x,t)\to -u_\nu(\pi-x,t)$ leaves (1) invariant (or statistically invariant) if $\sigma(\pi-x)=-\sigma(x)$ [or $=\sigma(x)$] holds; in these cases, therefore, stationary averages of $u_\nu(x,t)$ must be invariant under the inversion by the uniqueness of the stationary state.

Assume $\sigma(x)=(2/\pi)^{1/2}\sin x$ again. By the motion of zeros discussed in Sec. II B and by the correspondence between (signs of) $P(t)$ and groups of profiles shown in Fig. 1, the random motion of $u_\nu(x,t)$ for $\nu\sim +0$ may be grasped as separating into three clusters (structures) of profiles, each cluster being centered around the one depicted in Fig. 1. The birth process of $Z(t)$ mentioned in Sec. II B and the above-concluded ergodicity further indicate that the global structure of the motion of $u_\nu(x,t)$ for $\nu\sim +0$ consists of random but unbiased itineration among these clusters, which may schematically be denoted as (b) $\to\{{}^{(a)}_{(c)}\}\to$(b)$\to\{{}^{(a)}_{(c)}\}\to$(b)$\to\cdots$.

It is now our aim to draw more quantitative conclusions from this picture and question how the picture itself can be extended to more general cases of $\sigma(x)$. To this end we turn in Secs. III and IV to an approximation on (1) that admits analytic forms for its solutions.

III. THE MODEL

Consider the temporally stationary state of $u_\nu(x,t)$ for $s\downarrow-\infty$, and let $\langle\ \rangle$ denote the average in this state. Introduce

$$U_\nu(x)\equiv\langle u_\nu(x,t)\rangle, \quad \hat{u}_\nu(x,t)\equiv u_\nu(x,t)-U_\nu(x) . \qquad (16)$$

There hold

$$\tfrac{1}{2}d[U_\nu^2(x)+\langle \hat{u}_\nu^2(x,t)\rangle]/dx = \nu d^2U_\nu/dx^2 , \qquad (17)$$

$$\partial\hat{u}_\nu(x,t)/\partial t+\partial[U_\nu\hat{u}_\nu+\tfrac{1}{2}(\hat{u}_\nu^2-\langle\hat{u}_\nu^2\rangle)]/\partial x = \nu\partial^2\hat{u}_\nu/\partial x^2+\sigma(x)f(t) . \qquad (18)$$

We approximate (18) by discarding the self-convection term $\frac{1}{2}\partial(\hat{u}_\nu^2-\langle\hat{u}_\nu^2\rangle)/\partial x$ of the fluctuation. Since the resulting equations give solutions different from $\{U_\nu,\hat{u}_\nu\}$, we write

$$v_\nu(x,t)=V_\nu(x)+\hat{v}_\nu(x,t) , \qquad (19)$$

$$\tfrac{1}{2}d[V_\nu^2(x)+\langle\hat{v}_\nu^2(x,t)\rangle]/dx=\nu d^2V_\nu/dx^2 , \qquad (20)$$

$$\partial\hat{v}_\nu/\partial t+\partial(V_\nu\hat{v}_\nu)/\partial x=\nu\partial^2\hat{v}_\nu/\partial x^2+\sigma(x)f(t) , \qquad (21)$$

$$E_\nu(x)\equiv C_\nu(x,x), \quad C_\nu(x,y)\equiv\langle\hat{v}_\nu(x,t)\hat{v}_\nu(y,t)\rangle . \qquad (22)$$

This approximation enjoys solvability in the limit $\nu\downarrow 0$. In this sense we call $v_\nu(x,t)$ a model of $u_\nu(x,t)$. There holds

$$\partial v_\nu/\partial t+\partial(\langle v_\nu\rangle v_\nu+\tfrac{1}{2}\langle v_\nu^2\rangle-\langle v_\nu\rangle^2)/\partial x = \nu\partial^2 v_\nu/\partial x^2+\sigma(x)f(t) . \qquad (23)$$

Thus $v_\nu(x,t)$ gives a mean-field approximation of (1) that resembles the Weiss approximation in the Ising problem in some respects. It was derived[8] as the first nontrivial truncation of Wiener-Itô decomposition of $u_\nu(x,t)$ by multiple Wiener integrals over $\{f(t');s\leqq t'\leqq t\}$.[14,15]

As already mentioned, the self-convection constructs on the field $u(x,t)\equiv u_{+0}(x,t)$ shock discontinuities that satisfy the entropy condition, and we should look for typical samples of the t-homogeneous $u(x,t)$ in the class of functions of x with bounded variations.[4-6] Such a general guiding rule is not known for the inviscid limit of (23). We therefore *define* the model in the spirit of the boundary layer approximation. Equation (23) will be considered first with small but positive ν that will give $v_\nu(x,t)$ with all differentiabilities in x. Consider the temporally stationary state of this $v_\nu(x,t)$ for $s\downarrow-\infty$. By the linearity of (21), $v_\nu(x,t)$ has the form

$$\hat{v}_\nu(x,t)=\int_{-\infty}^{t}K(x,t-s)f(s)ds , \qquad (24)$$

$$\partial K(x,t)/\partial t+\partial[V_\nu(x)K(x,t)]/\partial x=\nu\partial^2K/\partial x^2 ,$$

$$K(x,+0)=\sigma(x) . \qquad (25)$$

These yield

$$C_\nu(x,y)=\int_0^\infty K(x,t)K(y,t)dt\ ,$$

$$\partial[V_\nu(x)C_\nu(x,y)]/\partial x+\partial[V_\nu(y)C_\nu(x,y)]/\partial y = \nu\Delta C_\nu(x,y)+\sigma(x)\sigma(y)\ , \quad (26)$$

$$\Delta\equiv\partial^2/\partial x^2+\partial^2/\partial y^2\ .$$

Equations (20) and (26) form an elliptic system with boundary conditions

$$V_\nu(x)\,|_{\partial X}=C_\nu(x,y)\,|_{\partial(X\times X)}=0\ . \quad (27)$$

Elliptic boundary value problems with small coefficients in the highest order derivatives often yield solutions with boundary layers.[16] Therefore, $V_\nu(x)$ and $C_\nu(x,y)$ for $\nu\sim+0$ will consist of parts well approximated by the inviscid solutions of (20) and (26) without terms $\nu d^2V_\nu/dx^2$ and $\nu\Delta C_\nu$. These inviscid solutions will cover the most parts of spaces X and $X\times X$. However, not all of boundary conditions (27) can be satisfied by inviscid solutions. There will arise thin boundary layers in which [as in shock fronts (5)] $\nu d^2V_\nu/dx^2$ and $\nu\Delta C_\nu$ show recognizable magnitude even for $\nu\sim+0$. The whole solution $\{V_\nu,C_\nu\}$ will be determined without ambiguity by matching inviscid and boundary layer solutions so that (27) is fulfilled.

IV. STATIONARY SOLUTIONS OF THE MODEL

A. Closed solutions of the model

The above type of solutions for (23) with $\nu\sim+0$ exist in closed forms for the stationary state. Their forms are summarized below.

Theorem. Let $\sigma(x)$ fulfill (2) and (4) with Hölder continuous $\sigma''(x)$. Temporally stationary solutions of (23) with boundary layer structures for $V_\nu(x)$ and $C_\nu(x,y)$ exist for $\nu\sim+0$. The solutions are not unique, with their multiplicities depending on $\sigma(x)$. Denote $V(x)\equiv V_{+0}(x)$, $E(x)\equiv E_{+0}(x)$, $C(x,y)\equiv C_{+0}(x,y)$, and $v(x,t)\equiv v_{+0}(x,t)$, limits for $\nu\downarrow0$ being defined as inviscid solutions determined by the boundary layer matching. All solutions satisfy

$$\langle v^2(x,t)\rangle=\langle v^2(x,t)\rangle_T=V^2(x)+E(x)=\gamma_n^2\ ,$$
$$\gamma_n\equiv(3/n)^{1/3}\times2^{-5/6}\ , \quad (28)$$

where $\langle A(t)\rangle_T$ is the time average,

$$\langle A(t)\rangle_T\equiv\lim_{s\downarrow-\infty}\frac{1}{t-s}\int_s^t A(r)dr\ ,$$

and $n\in\{\frac{1}{2},1,\frac{3}{2},2,\dots\}$ takes values proper to $\sigma(x)$. Explicit forms of $V(x)$, $E(x)$, and $\hat v(x,t)\equiv\hat v_{+0}(x,t)$ for a possible value of γ_n are given as follows with another proper value $\lambda\in X$ associated with $\sigma(x)$,

$$V(x)=2^{1/2}\gamma_n\sin\left[\tfrac{1}{3}\sin^{-1}\left(3\times2^{-3/2}\gamma_n^{-3}\int_\lambda^x\sigma^2(y)dy\right)\right]\ , \quad (29)$$

$$E(x)\equiv\langle\hat v^2(x,t)\rangle=\langle\hat v^2(x,t)\rangle_T=\gamma_n^2-V^2(x)\ , \quad (30)$$

$$\hat v(x,t)=\int_{-\infty}^t K(x,t-s)f(s)ds\ , \quad (31a)$$

$$K(x,t)=V(\chi(x,-t))\sigma(\chi(x,-t))/V(x)\ , \quad (31b)$$

$$\partial\chi(x,t)/\partial t=V(\chi(x,t)),\quad \chi(x,0)=x\ . \quad (31c)$$

Possible values of (n,λ) are exhausted by the following statements (a)—(c).

(a) The states with $n=\frac{1}{2}$ arise with any $\sigma(x)$ in doublet, with two possible values $\lambda=\pi$ and $\lambda=0$.

(b) Let λ be so defined that the ordinate $x=\lambda$ bisect the area below the graph of $\sigma^2(x)$ on X. For any $\sigma(x)$ there exists the state $(1,\lambda)$.

(c) If $\sigma(x)$ has zeros on $0<x<\pi$ and if these zeros satisfy some further restrictions, there arise other stationary states. Any of them consists of pieces of solutions (28)—(31c) on subintervals of X, all with the same $n\geqq1$ but corresponding to different λ's for this n.

We shall use a running index i and its symbolic values $\{a,b,c,\dots\}$ to denote pairs $(n,\lambda),(n',\lambda'),\dots$. The derivation of these solutions in the theorem requires some length for its description. We defer the details to Appendixes B and C for the compactness of the text. The above theorem refers only to pure states, so to speak, of the stationary solutions of (23). Since there exist at least three such pure states $a\equiv(\frac{1}{2},\pi)$, $b\equiv(1,\lambda)$ with λ of (b), and $c\equiv(\frac{1}{2},0)$ for any $\sigma(x)$, mixtures of states may always be constructed. The following gives their description in an obvious way.

Corollary. Let $i\in I\equiv\{a,b,c,\dots\}$ specify pure states in the theorem, respectively, with the probability measure $dP_i(\omega)$ on the probability space Ω $(\in\omega)$ of the Gaussian white noise. Let $I\times\Omega$ be the product space of (i,ω), and let $p_i\geqq0$ satisfy $\sum_{i\in I}p_i=1$. The probability measure on $I\times\Omega$,

$$dP(i,\omega)\equiv p_i\,dP_i(\omega)\ , \quad (32)$$

for any such $\{p_i\}$ defines a stationary solution of the following version of (23):

$$\partial v_\nu/\partial t+\partial(\langle v_\nu\rangle_T v_\nu+\tfrac{1}{2}\langle v_\nu^2\rangle_T-\langle v_\nu\rangle_T^2)/\partial x = \nu\partial^2v_\nu/\partial x^2+\sigma(x)f(t)\ , \quad (23')$$

as a mixture of pure states.

B. Statistics

We take $\sigma(x)=(2/\pi)^{1/2}\sin x$ as the representative of $\sigma(x)\neq0$ on $0<x<\pi$. By (a)—(c) of the theorem there are only three pure states, $I=\{a,b,c\}$ in the previous notation. The symmetry stipulates that $a=(\frac{1}{2},\pi)$ and $c=(\frac{1}{2},0)$ are inversions $v(x,t)\to-v(\pi-x,t)$ of each other, with $b=(1,\pi/2)$. Figure 4 gives the average $V(x)$ and the variance $E(x)$ of these pure states, respectively, with ordinates exhibiting ±1 by their length. For the rest of this subsection, we shall use notations $V_i(x)\equiv\langle v(x,t)\rangle_i$ and $E_i(x)\equiv\langle\hat v^2(x,t)\rangle_i\equiv\langle[v(x,t)-V_i(x)]^2\rangle_i$ with $i\in I$, where $\langle\ \rangle_i$ specifies the expectation in the pure state i.

Average profiles $V_a(x)-V_c(x)$ in Fig. 4(a)—(c) are reminiscent of the centering profiles of Fig. 1(a)—(c), respectively. We naturally inquire on the construction of a mix-

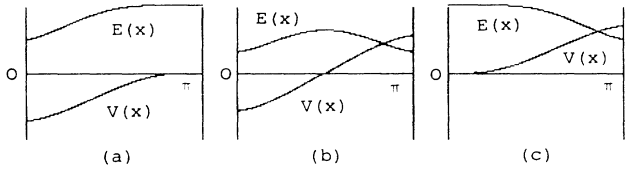

FIG. 4. Average and variance profiles of pure states of the model for $\sigma(x)=(2/\pi)^{1/2}\sin x$.

ture of these pure states, choosing hopefully p_a-p_c of the corollary for relative sojourn times of u_ν in these structures and aiming at the reproduction of the statistics of u_ν. To proceed, we first compare profiles in the pure state b with numerical results for (1), taken from a run for the same $\sigma(x)$ with $\nu=(2/\pi)^{1/3}/50=0.0172$ up to $t=73.74$. Further details of this numerical process are given in Sec. V.

Figures 5 shows $V_b(x)$ and $U_\nu(x)\equiv u_\nu(x,t)\rangle_T$, $E_b(x)$, and $E_\nu(x)\equiv\langle\hat{u}_\nu^{\,2}(x,t)\rangle_T$, skewness factors

$$S_b(x)\equiv\langle\hat{v}^{\,3}(x,t)\rangle_b/E_b^{3/2}(x)\equiv 0\ ,$$

$$S_\nu(x)\equiv\langle\hat{u}_\nu^{\,3}\rangle_T/E_\nu^{3/2}(x)\ ,$$

and normalized flatness factors

$$F_b(x)\equiv\tfrac{1}{3}\langle\hat{v}^{\,4}\rangle_b/E_b^2(x)\equiv 1\ ,$$

$$F_\nu(x)\equiv\tfrac{1}{3}\langle\hat{u}_\nu^{\,4}\rangle_T/E_\nu^2(x)\ .$$

All ordinates stand for the interval $[-1,1]$. The divergence of $S_\nu(x)$ and $F_\nu(x)$ is due to the rapid decrease of normalizing $E_\nu(x)$ as $x\to 0$ and $x\to\pi$, and goes closer to walls as $\nu\downarrow 0$. Though this pure state b in isolation can never reproduce non-Gaussian behaviors of $u_\nu(x,t)$, (23′) is kinematically a natural approximation of (1) insofar as we collect only motions of u_ν around the centering profile of Fig. 1(b) with small deviations. We thus turn to the question of how the other two pure states can be mixed to fill up the remaining motions of $u_\nu(x,t)$. In passing we note the following. There holds $E_b(\pi-0)=\gamma_1^2/2=V_b^2(\pi-0)>0$. Therefore, 15.9% of (Gaussian) samples of $v(x,t)$ in the pure state b with $\hat{v}(\pi-0,t)<-\gamma_1/2^{1/2}$ violate the entropy condition $v(\pi-0,t)\geqq 0$. The matter is

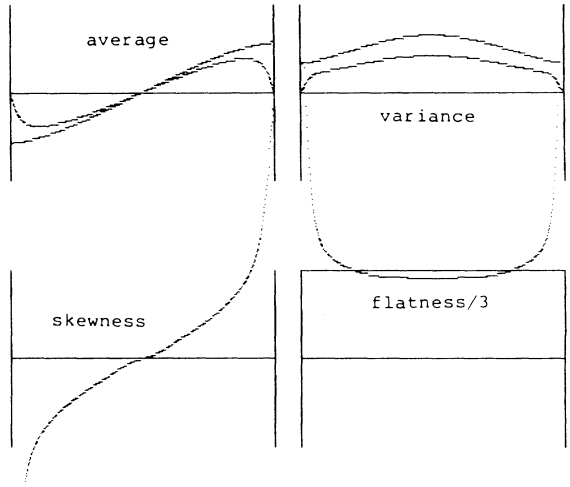

FIG. 5. Profiles of numerical results and the model pure state b for $\sigma(x)=(2/\pi)^{1/2}\sin x$.

the same at $x=+0$. This figure 0.159 will give a measure of quantitative accuracy of this state b as an approximation of the mentioned portion of samples of $u_\nu(x,t)$.

For convenience we next take the mixture, to be denoted ac, for $p_a=p_c=\frac{1}{2}$ and $p_b=0$ in the corollary. Denote $\langle\ \rangle_{ac}$ for the average with respect to (32) of this mixture ac, and define $\tilde{v}\equiv v-V_{ac}$ with $V_{ac}(x)\equiv\langle v(x,t)\rangle_{ac}$. Figures 6 shows, with the same numerical results as Fig. 5, profiles of the average $V_{ac}(x)$, the variance $E_{ac}(x)\equiv\langle\tilde{v}^{\,2}(x,t)\rangle_{ac}$, and skewness and normalized flatness factors $S_{ac}(x)\equiv\langle\tilde{v}^{\,3}\rangle_{ac}/E_{ac}^{3/2}(x)$ and $F_{ac}(x)\equiv\frac{1}{3}\langle\tilde{v}^{\,4}\rangle_{ac}/E_{ac}^2(x)$. The accuracy of this solution will be discussed shortly.

We are now in a position to examine a further mixture, to be called the ϵ mixture with its expectations to be denoted $\langle\ \rangle_\epsilon$, giving the probability ϵ to Fig. 5 and $1-\epsilon$ to Fig. 6; this is just the mixture $p_a=p_c=(1-\epsilon)/2$ and $p_b=\epsilon$ of the corollary. Denoting $V_\epsilon(x)$, $E_\epsilon(x)$, $S_\epsilon(x)$, or $F_\epsilon(x)$ for the average, the variance, the skewness factor, or the normalized flatness factor in this mixture, respectively, we have

$$V_\epsilon(X)=\epsilon V_b(x)+(1-\epsilon)V_{ac}(x)\ , \tag{33}$$

$$E_\epsilon(x)=\epsilon E_b(x)+(1-\epsilon)E_{ac}(x)+\epsilon(1-\epsilon)\Xi^2(x),\quad \Xi(x)\equiv V_b(x)-V_{ac}(x)\ , \tag{34}$$

$$S_\epsilon(x)=(1-\epsilon)S_{ac}(x)e_{ac}^{3/2}(x)+\epsilon(1-\epsilon)\xi(x)[3e_b(x)-3e_{ac}(x)+(1-2\epsilon)\xi^2(x)]\ , \tag{35}$$

$$\xi(x)\equiv\Xi(x)/E_\epsilon^{1/2}(x),\quad e_b(x)\equiv E_b(x)/E_\epsilon(x),\quad e_{ac}(x)\equiv E_{ac}(x)/E_\epsilon(x)\ , \tag{36}$$

$$F_\epsilon(x)=\epsilon e_b^2(x)+(1-\epsilon)F_{ac}(x)e_{ac}^2(x)+\epsilon(1-\epsilon)\xi(x)\{(1-3\epsilon+3\epsilon^2)\xi^3(x)+6[(1-\epsilon)e_b(x)+\epsilon e_{ac}(x)]\xi(x)-4S_{ac}(x)e_{ac}^{3/2}(x)\}. \tag{37}$$

Figures 5 and 6 show the ordering $V_{ac}(x)\lesssim U_\nu(x)\lesssim V_b(x)$ on the main portion of $0<x<\pi$. Therefore, $V_\epsilon(x)$ of (33) can be made very close to $U_\nu(x)$ by a suitable choice of $\epsilon>0$. As to the variance $E_\epsilon(x)$, however, the matter is not prosperous. From figures we see $E_\nu(x)<E_b(x)\ll E_{ac}(x)$; $E_\epsilon(x)$ of (34) can never be closer to $E_\nu(x)$, even at $x=\pi/2$ that gives $\Xi^2(x)=0$, than $E_b(x)$ whatever $0\leqq\epsilon\leqq 1$ may be.

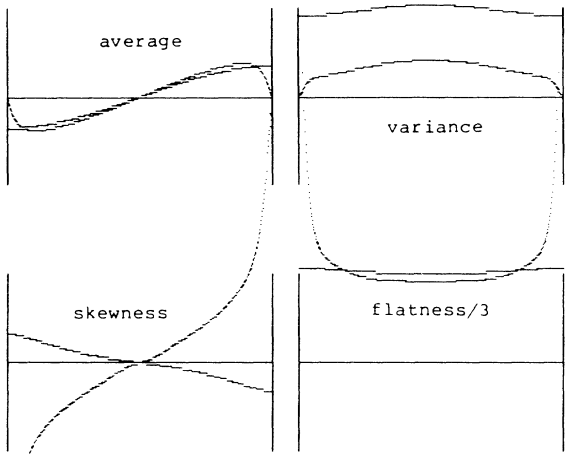

FIG. 6. Profiles of numerical results and the model mixture $a+c$ for $\sigma(x)=(2\pi)^{1/2}\sin x$.

Since $E_b(x)$ is expected to represent a definite portion of the reality of $u_\nu(x)$, the above observation stipulates that $E_{ac}(x)<E_\nu(x)$ must hold, if the mixture ac should approximate the remaining portion of $u_\nu(x,t)$. This necessity is also seen from other respects: The existence of a centering profile of the type of Fig. 1(c) implies that fluctuations given to the fluid at $x\sim\pi/2$ are more promptly convected and deposited than the case of Fig. 1(b), while the entropy condition prohibits stringently positive fluctuations at the stagnant portion $x\sim 0$. In contrast, the model has $E_c(+0)=\gamma_{1/2}^2>0$ with $V_c(+0)=0$; 50% of samples of $v(x,t)$ in the pure state c violate the entropy condition at $x\sim 0$. The reader is asked to refer to Appendix B for the origin of this fault. Unluckily, these samples of $v(x,t)$ of poor quality, which occupy the shaded portion at $x\sim 0$ in the schematic Fig. 7, give the largest values to $\tilde{v}(x,t)=v(x,t)-V_{ac}(x)$. The matter is the same with the pure state a at $x\sim\pi$.

The above observations suggest a direction[17] to which pure states a and c should be improved. We circumvent this difficult way, however, and close this section promptly by presenting a prospect: The modification on states a and c can in fact give consistent statistics that reproduce higher degree moments of $u_\nu(x,t)$, at least where one-time expectation values are concerned. Consider the simple case that model pure states a and c consists of deterministic samples $v(x,t)\equiv\bar{V}_i(x)$, $i=a$ or c. Their even mixture gives $V_{ac}(x)=[\bar{V}_a(x)+\bar{V}_c(x)]/2$, $E_{ac}(x)=[\bar{V}_a(x)-\bar{V}_c(x)]^2/4$, $S_{ac}(x)\equiv 0$, and $F_{ac}(x)\equiv\frac{1}{3}$. Assume[17] $\bar{V}_{ac}(x)<V_b(x)$ on $\pi/2<x<\pi$ and $E_{ac}(x)<E_b(x)$. Equations (33)—(37) assure that $V_\epsilon(x)$ can be close to $U_\nu(x)$, and that $E_\epsilon(x)$ is diminished from $E_b(x)$ at $x=\pi/2$ and flattened for $x\to 0$ or π by E_{ac} and Ξ^2 terms. There also holds

$$S_\epsilon(x)=\epsilon(1-\epsilon)\xi(x)\{3[e_b(x)-e_{ac}(x)]+(1-2\epsilon)\xi^2(x)\},$$

which is positive on $\pi/2<x<\pi$ for $\epsilon<\epsilon_1$ with certain $\epsilon_1>\frac{1}{2}$. The matter is intricate with $F_\epsilon(x)$, but it is continuous in ϵ with $F_\epsilon(x)|_{\epsilon=0}=F_{ac}(x)=\frac{1}{3}\ll 1$. Thus $S_\epsilon(x)=-S_\epsilon(\pi-x)>0$ on $\pi/2<x<\pi$ and $F_\epsilon(x)<1$ hold for $\epsilon<\epsilon_2$, with certain $\epsilon_2>0$. These are the tendencies of numerical results shown in Fig. 5 or Fig. 6.

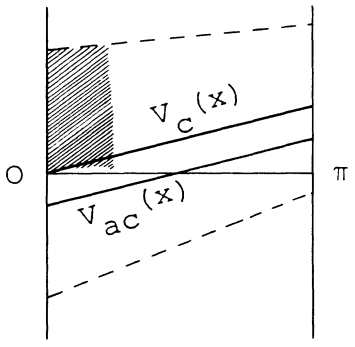

FIG. 7. Schematic distributions of profiles in the model pure state c on $0\leqq x\leqq\pi$.

V. NUMERICAL RESULTS

Some details are now described on the adopted numerical procedures and their results. In solving (1)—(4) numerically, advantages were taken of the known $L^1(X)$ convergence of $u_\nu(x,t)$ for $\nu\downarrow 0$ by choosing small but positive ν's that facilitate the processes. The spatial mesh size was chosen exclusively as $\Delta x=\pi/500$. The time steps were $\Delta t=O(\pi/10^4)$, varying slightly with runs. The explicit difference scheme of Lax[18] was adopted by its two merits: [1] It gives a stable discretization of the linear diffusion term, and [2] the explicitness of the scheme enables nonanticipating[10] construction of solutions. This scheme gives[18] $\nu=(\Delta x)^2/(2\Delta t)=O(\pi/50)$, which implies that a shock front of (5) of a width of $O(\nu)$ contains at least ten mesh points of x, and cannot be overlooked. Runs were in double precision. For the free decay $\sigma(x)\equiv 0$ it was confirmed with the initial data $\psi(x)=-\sin(2x)$ and $\Delta t=\pi/10^4$ (i.e., $\nu=\pi/50$) that the momentum is conserved $[P(t)\equiv 0]$ and the half-life T of the profile is $T\cong 3000\Delta t=O(1)$, T being defined by the half-decay of the total energy $E(t)$.

The main runs were performed with $\sigma(x)=(2/\pi)^{1/2}\sin(2x)$ for[19] $\psi(x)=-\alpha\sin(2x)$, $\alpha=(2/\pi)^{1/3}$, $\Delta t=\pi/(10^4\alpha)$, and $\nu=\alpha\pi/50$. As already mentioned, the evolution of profiles showed the simple correspondence between $P(t)\lessgtr 0$ and the types of profiles of Fig. 1(a)—1(c), respectively, and also the sole possible way of birth of new zeros on a profile as depicted in Fig. 2 or its inversion. As the typical and outright data showing this appearance of distinct clusters of profiles, we give in Fig. 8(a) sample behavior of the total momentum $P(t)$ in a long run up to $t=44.17$, together with the total energy and its time average, and the momentum input $W(t)=\Sigma B(t)=\Sigma\int_0^t f(s)ds$. Here $W(t)$ is chopped at equal time intervals and recommenced from 0 in order to avoid its divergence $\propto\Sigma t^{1/2}$. All ordinates of these graphs show ± 3 or 3 in respective units. The distribution of values of $P(t)$, taken at every ten time steps, is drawn

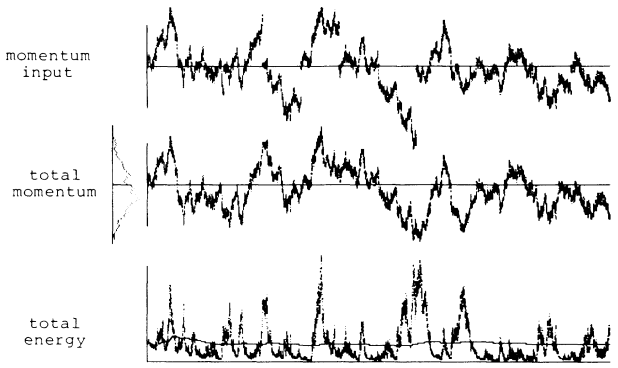

FIG. 8. Realized time evolutions of a long numerical run for $\sigma(x) \propto \sin x$.

as a density on the left of the $P(t)$ graph in the same scale, showing three peaks at $P \simeq 0.8$, 0, and -1.[20] This confirms, along with the correspondence between $P(t)$ and Fig. 1(a)—1(c), the existence of three clusters of profiles as discussed from analytic viewpoints in Sec. II.

The distribution of $P(t)$, however, shows scatter with runs. In another long run up to $t=73.74$, peaks were at approximately 0.8, 0, and -0.4. Both of the mentioned distributions of $P(t)$ show asymmetry at $P=0$. These imply that the convergence of time averages is not yet attained, indicating the slowness of convergence and also the strength of the lingering property of profiles in quasistationary structures. By the inpracticability of longer numerical runs,[21] Figs. 5 and 6 show time-average profiles that are (anti-) symmetrized at $x=\pi/2$.

Finally we note the following. If $\sigma(x) \propto \sin(2x)$ holds, (1) admits solutions that are inversion invariant for $\forall t \geqq s$. The unique stationary state of (1) should thus be composed of such samples. For the same $\sigma(x)$, the model (23) can have three pure states, $a'=(1,\pi 2)$, $b'=(2,\pi/4)$, and $c'=(1,0)$, which represent (a) and (b) of the theorem for the problem on $0 \leqq x \leqq \pi/2$ and which should be extended antisymmetrically (by inversion) to $\pi/2 \leqq x \leqq \pi$. Besides these, the model also has pure states $a=(\frac{1}{2},\pi)$ and $c=(\frac{1}{2},0)$, $b=(1,\pi/2)$ being identical to a'. These a and c break the antisymmetry of the problem at $x=\pi/2$, and they are spurious as approximations of (1). When $\sigma(x) \propto \sin(2x)+\epsilon \sin x$ holds with small $|\epsilon|$, however, the model (23) can have only pure states a—c, lacking solutions that correspond to b' and c'. Therefore, a question arises what will occur on (1) for this $\sigma(x)$. A numerical run was thus performed with $\sigma(x) = (1.09\pi/2)^{-1/2}[\sin(2x)+0.3\sin x]$ for $\Delta t=\pi/(10^4\beta)$ and $\nu=\beta\pi/50$, where $\beta=(1.09\pi/2.06)^{-2/3}$. The result was simply that $u_\nu(x,t)$ shows behaviors that are inferable continuously from the case of $\sigma(x) \propto \sin(2x)$. The model fails to reproduce moving shock fronts, which show up on samples of $u_\nu(x,t)$ at $x \sim \pi/2$ continually. Luckily, this fault of the model was of little relevance with $\sigma(x) \propto \sin x$ for which such a moving shock front appears only rarely and only near walls associated with the process sketched in Fig. 3. If we should construct approximations of (1) with the model for problems that are slightly off the case of inversion invariance, a perturbative approach will be adequate, starting from the case of complete antisymmetry.

VI. CONCLUDING REMARKS

We have discussed, both analytically and numerically, the forced motion of Burgers fluid between walls in the inviscid limit. As regards the case $\sigma(x) \neq 0$ on $0<x<\pi$ for the problem (1)—(4), the motion shows a strong resemblance to Brownian motion in triply bottomed potentials. This has long been speculated[8] by the discovery of the model and its closed solutions. Sorry to say, a misconception has intervened on the basic role of the pure state b in these works, and the point was appreciated correctly only after the very recent numerical runs.

For a slightly more general problem with $\sigma(x)$ that can have points of approximate antisymmetry,[13] numerical results suggest the general tendency that shock fronts can continually be formed in (selected sets of) vicinities of these points, giving spatial configurations for the dissipation among which the system will itinerate. A sojourn time of u_ν in such a quasistationary structure can be very long, but it can also be only transitory,[22] as seen in the $P(t)$ graph of Fig. 8. This causes another inaccuracy in (23′), as an approximation for (1).

The $L^1(X)$ stability (13) of $u_\nu(x,t)$, which persists even at $\nu=+0$, shows apparently a distance from the usual turbulence phenomena that are stochastic not only by the randomness in the force but by instabilities in their dynamics. In (1), however, not all instabilities are ruled out by (13). In order to have perspectives on this point, we consider the BV norm $||q(x)||_{\mathrm{BV}}$ defined by the total variation[23] of $q(x)$ on X. Assume[13] by (2) that all functions of x are centered at their discontinuities, $q(x) \equiv \frac{1}{2}[q(x-0)+q(x+0]$. Let $\psi(x)$ be in the space $\mathrm{BV}(X)$ of (centered) functions of bounded variations equipped with the BV norm: $\mathrm{BV}(X)$ forms the dual space of $C^0(X)$. For any $0<\nu \leqq 1$ and $s \leqq t \leqq \forall T < \infty$ there hold (ν,t)-independent estimates on $||u_\nu(x,t;\psi)||_{\mathrm{BV}}$ and the $L^1(X)$ modulus of continuity of $u_\nu(x,t;\psi)$ in t; cf. Ref. 4, Sec. 2, lemma 1. These facts and $L^1(X)$ convergence for $\nu \downarrow 0$ of $u_\nu(x,t;\psi)$ assure that $u_\nu(x,t;\psi) \in [C^0(X)]^*$ is weakly* continuous in $(\nu,t) \in [0,1] \times [s,T]$. In other words, an arbitrary $q(x) \in C^0(X)$ gives a (ν,t)-continuous Stieltjes integral $\int_X q(x) du_\nu(x,t;\psi)$, which is $-\int_X q'(x) u_\nu(x,t;\psi) dx$ for $q(x) \in C^1(X)$ by (2).

The motion of $u(x,t;\psi)$ in $\mathrm{BV}(X)$ is not norm-continuous for general $\psi(x) \in \mathrm{BV}(X)$, as seen in the second example below. Correspondingly, $u(x,t;\psi)$ in $\mathrm{BV}(X)$ can show behaviors which are qualitatively quite different from the indication of (13). As the first example showing this, we take ψ and ψ^* of Fig. 9 and define $d(t;\psi,\psi^*) \equiv ||u(x,t;\psi)-u(x,t;\psi^*)||_{\mathrm{BV}}$. In the free evolution for $\sigma(x) \equiv 0$ we have[5] $d(s+\tau;\psi,\psi^*)=2\epsilon/(\frac{1}{2}-\tau)$ for $0 \leqq \tau \leqq \frac{1}{2}-\epsilon$. However small $d(s;\psi,\psi^*)=4\epsilon$ may be, it attains the value 2 independent of ϵ after a finite lapse of time at which a shock discontinuity is built on $u(x,t;\psi^{(*)})$. As the second example, we consider $\psi(x)$ with a shock discontinuity at $x=S$ that is not a center of

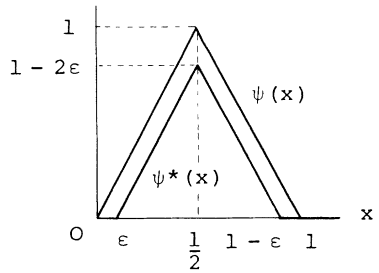

FIG. 9. Two initial data showing time-local BV(X) instability.

inversion invariance. If $\psi^*(x)$ has the same location $x=S$ for its own discontinuity with $\psi^*(S-0)=\psi(S-0)-\epsilon$ and $\psi^*(S+0)=\psi(S+0)$, $d(s;\psi,\psi^*)=O(\epsilon)$ jumps to a different, essentially ϵ-independent value at $\forall t>s$ by (6). These space-time local behaviors persist in the forced case.

If $\sigma(x)$ admits points of approximate antisymmetry, the force will continually generate moving shock discontinuities on a typical sample of $u(x,t)$ in the stationary state. Further, quantities of the type[23] of $|\partial u(x,t)/\partial x|$ are often the objects of physical concern—for example, as the enstrophy in Navier-Stokes problems. The circumstance suggests not only that Burgers fluid for $\nu\cong+0$ can serve as models of some turbulence phenomena despite (13), but also that the motion of Burgers or more general fluids can be chaotic or orderly depending on what quantities we aim physically, and are in fact able, to observe on it.[24]

ACKNOWLEDGMENTS

The author thanks Hideki Takayasu for helpful discussions on, and for some facilities in, numerical procedures in this work.

APPENDIX A

Let $\epsilon(\tau)$ be a rapidly decreasing function for $\tau\to\pm\infty$, and introduce the smeared Gaussian white noise $f_\epsilon(t)$:

$$f_\epsilon(t)=\int_{-\infty}^{\infty}\epsilon(t-s)f(s)ds,\quad \langle f_\epsilon(t)\rangle=0\ , \tag{A1}$$

$$\langle f_\epsilon(t)f_\epsilon(t+\tau)\rangle=\int_{-\infty}^{\infty}\epsilon(\tau+\tau')\epsilon(\tau')d\tau'\equiv\delta_\epsilon(\tau)\ .$$

Samples of $f_\epsilon(t)$ may be taken differentiable any number of times, and Eq. (1) with its $f(t)$ replaced by $f_\epsilon(t)$ may be defined samplewise as a usual (nonstochastic) forced Burgers equation. This gives that samples of $u_\nu(x,t)$ have all differentiabilities in x and t, and $u_\nu(Z(t),t)=0$ implies

$$Z'(t)=-\nu G_x(Z(t),t)-f_\epsilon(t)H(Z(t),t)\ ,$$

$$G(x,t)\equiv\ln u'_\nu(x,t),\quad H(x,t)\equiv\sigma(x)/u'_\nu(x,t)\ .$$

For simplicity we take that the conditioning is given at $t=0$. We also use momentarily the abbreviated notations

$$G_x(t)=G_x(Z(t),t),\quad H(t)=H(Z(t),t)\ ,$$
$$H_x(t)=H_x(Z(t),t),\quad H_t(t)=H_t(Z(t),t)\ ,$$
$$U_x(t)=u'_\nu(Z(t),t),\quad U_{xx}(t)=u''_\nu(Z(t),t)\ ,$$
$$U_{xxx}(t)=u'''_\nu(Z(t),t),\quad \Sigma(t)=\sigma(Z(t))$$
$$\Sigma'(t)=\sigma'(Z(t))\ .$$

Finally, we choose a small but finite $\tau>0$, and evaluate the time average $\tau^{-1}\int_0^\tau\langle Z'(t)\rangle_c dt$, toward the limit $\tau\downarrow0$. The following iteration is useful to this end:

$$\begin{aligned}H(t)&=H(0)+\int_0^t H'(s)ds\\&=H(0)+\int_0^t[H_x(s)Z'(s)+H_t(s)]ds\\&=H(0)+\int_0^t ds\,f_\epsilon(s)[-2\Sigma(s)\Sigma'(s)/U_x^2(s)+\Sigma^2(s)U_{xx}(s)/U_x^3(s)]\\&\quad+\int_0^t ds[-\nu\Sigma'(s)U_{xx}(s)/U_x^2(s)+\nu\Sigma(s)U_{xx}^2(s)/U_x^3(s)-\nu\Sigma(s)U_{xxx}(s)/U_x^2(s)+\Sigma(s)]\ .\end{aligned} \tag{A2}$$

Finally, we observe the general relation

$$\left\langle f_\epsilon(\tau)\int_0^t ds\int_0^s dr\,f_\epsilon(r)\right\rangle=O\left[\tau\int_{-\infty}^{\infty}\delta_\epsilon(\tau')d\tau'\right],\quad 0\leqq\forall t\leqq\tau\ ,$$

$$\left\langle f_\epsilon(\tau)\int_0^\tau dt_1\cdots\int_0^\tau dt_{2n-1}f_\epsilon(t_1)\cdots f_\epsilon(t_{2n-1})\right\rangle=(2n-1)!!\left[O\left[\tau\int_{-\infty}^{\infty}\delta_\epsilon(\tau')d\tau'\right]\right]^{n-1},\quad n=1,2,\cdots\ .$$

In total, we have

$$\tau^{-1}\int_0^\tau\langle Z'(t)\rangle_c dt=-\nu\tau^{-1}\int_0^\tau\langle G_x(t)\rangle_c dt-\tau^{-1}\int_0^\tau dt\int_0^t ds\langle f_\epsilon(t)f_\epsilon(s)\rangle$$
$$\times\langle-2\Sigma(s)\Sigma'(s)/U_x^2(s)+\Sigma^2(s)U_{xx}(s)/U_x^3(s)\rangle_c ds+O(\tau)\ ,$$

which in the limit $\delta_\epsilon(\tau)\to\delta(\tau)$ tends to the following by $\delta_\epsilon(-\tau)=\delta_\epsilon(\tau)$:

$$\tau^{-1}\int_0^\tau \langle Z'(t)\rangle_c dt=\tau^{-1}\int_0^\tau \langle F(Z(t),t)\rangle_c dt+O(\tau)\ .$$

Since the limit $\tau\downarrow 0$ gives $\langle F(Z(t),t)\rangle_c\to F(Z(0),0)$, we have the assertion.

APPENDIX B

Take $\nu\ll 1$. We look for the solutions of V_ν, E_ν, and C_ν with boundary layer parts and inviscid parts. We first discuss the forms of inviscid parts which are denoted as V, E, and C. Omitting the viscous term in (20), we obtain

$$V^2(x)+E(x)=\text{const}\equiv\gamma^2,\quad \gamma\geqq 0\ . \tag{B1}$$

Similarly, (26) with $x=y$ and without the viscous term yields

$$2V'(x)E(x)+V(x)E'(x)=\sigma^2(x)\ . \tag{B2}$$

These two equations are integrated to

$$J(V(x))=J(V(\lambda))+\Sigma(\lambda,x)\ , \tag{B3}$$

$$J(V)\equiv 2\gamma^2 V-\tfrac{4}{3}V^3,\quad \Sigma(\lambda,x)\equiv\int_\lambda^x \sigma^2(y)dy\ . \tag{B4}$$

Figure 10 shows the form of $J(V)$, together with a graphical way to obtain $V(x)$ with given values of λ and $V(\lambda)$. We restrict the arguments, for the time being, to the derivation of the solution $c=(\frac{1}{2},0)$ with $\lambda=0$ and $V(\lambda)=0$ assigned. From (B3) we obtain a third-degree algebraic equation for $V(x)$. The well-known method of solution with $\sin(\theta/3)$ gives the form of $V(x)$ in (29) for $\lambda=0$; (29) may also be confirmed by putting it into (B3), and it is valid generally for any pure states as well as $c=(\frac{1}{2},0)$. Since $\Sigma(\lambda,x)$ is monotonically increasing in x, Fig. 10 manifests the existence of the restriction

$$V(\pi)\leqq\gamma/2^{1/2}\ . \tag{B5}$$

Now we turn to the boundary layer needed for $V(x)$ of c, which fulfills $V(0)=0$, to fulfill the other boundary condition at $x=\pi$. Define the stretched coordinate ξ by $x=\pi+\nu\xi$ with $\xi<0$. Put

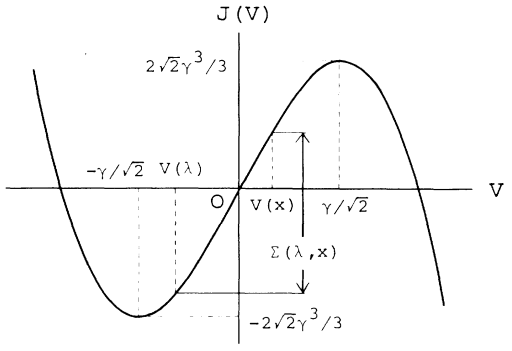

FIG. 10. A graphical method for the evaluation of $V(x)$.

$$V^*(\xi)\equiv V_\nu(\pi+\nu\xi)\ ,$$

$$K^*(\xi,t)\equiv K(\pi+\nu\xi,t)\ ,$$

$$E^*(\xi)\equiv E_\nu(\pi+\nu\xi)\ .$$

Equation (25) for $K(x,t)$ gives $\partial^2K^*/\partial\xi^2=\partial(V^*K^*)/\partial\xi$ for the leading terms. For $K^*(0,t)=0$ and for vanishing $\partial K^*/\partial\xi=\nu\partial K(x,t)/\partial x$ as $\xi\downarrow-\infty$, this has the following solution:

$$K^*(\xi,t)=k(t)\int_0^\xi d\eta\exp\left[\int_\eta^\xi V^*(\zeta)d\zeta\right]\ .$$

Here $k(t)$ is an arbitrary function. Putting this into $C_\nu(x,y)$ of (26), we obtain

$$C^*(\xi,\eta)\equiv C_\nu(\pi+\nu\xi,\pi+\nu\eta)=\phi(\xi)\phi(\eta),\quad E^*(\xi)=\phi^2(\xi)\ , \tag{B6}$$

$$\phi(\xi)=\left[\int_0^\infty k^2(t)dt\right]^{1/2}\int_0^\xi d\eta\exp\left[\int_\eta^\xi V^*(\zeta)d\zeta\right]\ .$$

By (B7) and by (26) for $x=y$, we have

$$d^2\phi/d\xi^2=d[V^*(\xi)\phi(\xi)]/d\xi\ . \tag{B7}$$

Equation (20) implies

$$d^2V^*/d\xi^2=\tfrac{1}{2}d[(V^*)^2+\phi^2]/d\xi\ . \tag{B8}$$

Addition and subtraction of (B7) and (B8) yield the following:

$$d^2\phi_\pm(\xi)/d\xi^2=\tfrac{1}{2}d\phi_\pm^2(\xi)/d\xi,\quad \phi_\pm(\xi)\equiv V^*(\xi)\pm\phi(\xi)\ . \tag{B9}$$

Take $\xi=-\nu^{-1/2}\ll-1$. This corresponds to $x=\pi-\nu^{1/2}\simeq\pi-0$. Therefore, $V^*(-\infty)$ and $\phi^2(-\infty)$ must be matched to finite values $V(\pi-0)$ and $E(\pi-0)$, respectively, of the inviscid solution. Examining $d^2\Phi/d\xi^2=\frac{1}{2}d\Phi^2/d\xi$ under the boundary conditions $\Phi(0)=0$ and $\Phi(-\infty)$ finite, we conclude that the possible form of $\Phi(\xi)$ on $-\infty<\xi<0$ is unique and given by $\Phi(\xi)=-\kappa\tanh(\kappa\xi/2)$, where $k\geqq 0$ is arbitrary. Thus we have the unique forms for $V^*(\xi)$ and $E^*(\xi)$,

$$\begin{aligned} V^*(\xi)&=-\kappa\tanh(\kappa\xi)-\kappa'\tanh(\kappa'\xi)\ ,\\ E^*(\xi)&=[\kappa\tanh(\kappa\xi)-\kappa'\tanh(\kappa'\xi)]^2\ , \end{aligned} \tag{B10}$$

where $\kappa\geqq\kappa'\geqq 0$ are constants. The matching conditions

$$V^*(-\infty)=\kappa+\kappa'=V(\pi-0)\leqq\gamma/2^{1/2}\ ,$$

$$E^*(-\infty)=(\kappa-\kappa')^2=\gamma^2-V^2(\pi-0)\geqq\gamma^2/2$$

imply the unique set of values $\kappa=\gamma/2^{1/2}$ and $\kappa'=0$. Thus we have

$$V(\pi-0)\equiv V_{+0}(\pi-0)=\gamma/2^{1/2}\ . \tag{B11}$$

This and (B3) give $J(\gamma/2^{1/2})=\Sigma(0,\pi)=1$, which determines $\gamma=\gamma_{1/2}$ given in (28). Using this value in (29) and (30), we complete the derivation of the temporally stationary state $c=(\frac{1}{2},0)$ for $V(x)$ and $E(x)\equiv E_{+0}(x)$, except for the point that $E(0)=(\gamma_{1/2})^2-V^2(0)>0$ seems to violate the fixed boundary condition for $E_\nu(0)$ without any boundary layer at $x=0$. In order to give some useful

view into the structure of the model solutions, we now go a little into this problem.

We observe (25) for the kernel $K(x,t)$ in the inviscid case:

$$\partial K/\partial t+\partial[V(x)K]/\partial x=0,\quad K(x,0)=\sigma(x)\ . \tag{B12}$$

The mean field $V(x)$ is monotonically increasing in x for the case $c=(\frac{1}{2},0)$, as shown in Fig. 4(c). The solution of (B12) is found by its characteristic equation (31c) for χ, and we obtain the form of K in (31b) which remans valid for any states other than c. At $x=0$ of the present case there holds $K(0,t)=0$. Therefore, the fluctuation $\hat{v}(x,t)$ constructed with this $K(x,t)$,

$$\hat{v}(x,t)=\hat{v}(x,s)+\int_s^t K(x,t-t')f(t')dt'\ , \tag{B13}$$

fulfills the boundary condition at $x=0$ if $\hat{v}(x,s)$ does. As the limit $s\downarrow-\infty$ of this expression, however, the integral for $E(x)$,

$$E(x)=\int_0^\infty K^2(x,t)dt=\int_0^x V(\chi)\sigma^2(\chi)d\chi/V^2(x)\ ,\qquad x>0$$

converges nonuniformly near $x=0$, and yields $E(+0)=(\gamma_{1/2})^2$ while $E(0)=0$. This implies that the limit $s\downarrow-\infty$ of $\hat{v}(x,t)$ of (31a) has a discontinuity, $\hat{v}(0,t)=0$, while $\hat{v}(x,t)\neq 0$ for $x>0$ with probability 1. We admit this type of discontinuous solution. See also some related descriptions below Fig. 7 in Sec. IV B for further implications of this feature of the model solution c as well as a.

The other stationary state $a=(\frac{1}{2},\pi)$ is obtained by the same procedure starting from $\lambda=\pi$ and $V(\pi)=0$. Finally we note that $\hat{v}(x,t)$ of (24) at a fixed $x\in X$ forms a stationary Gaussian process with mean zero and mutually independent $\hat{v}(x,t)$ and $\hat{v}(x,t+T)$ in the limit $T\to\pm\infty$ by the integrability of $K^2(x,t)$ in t. Thus $\hat{v}(x,t)$ is mixing. This justifies the replacement of the average of $f(t)$ with the long-time average, as in (28) or (30). This proves (a) of the theorem.

APPENDIX C

For the proof of (b) and (c) of the theorem, we first give a complete tabulation of the states referred to in theorem (c).

Theorem. (c*) Let $x_0\equiv 0<x_1<x_2<\ldots<x_p<x_{p+1}\equiv\pi$ be zeros of $\sigma(x)$ realizing one of the following four cases C_{p+1}, $C^0_{p+1/2}$, $C^\pi_{p+1/2}$, and $C^{0\pi}_p$, with $\Sigma(\lambda,x)$ of (B4):

C_{p+1}: $\Sigma(x_i,x_{i+1})=1/(p+1)$, $i=0,1,\ldots,p$, with the definition $\Sigma(x_j,\lambda_j)\equiv 1/[2(p+1)]$ for λ_j, $j=0,1,\ldots,p$, where $p=0,1,\ldots$.

$C^0_{p+1/2}$: $\Sigma(x_0,x_1)=1/(2p+1)$, $\Sigma(x_1,x_2)=\ldots=\Sigma(x_p,x_{p+1})=2/(2p+1)$, with the definition $\Sigma(x_j,\lambda_j)\equiv 1/(2p+1)$ for $j=1,\ldots,p$ where $p=0,1,\ldots$.

$C^\pi_{p+1/2}$: $\Sigma(x_0,x_1)=\ldots=\Sigma(x_{p-1},x_p)=2/(2p+1)$, $\Sigma(x_p,x_{p+1})=1/(2p+1)$, with the definition $\Sigma(x_j,\lambda_j)\equiv 1/(2p+1)$ for $j=0,1,\ldots,p-1$, where $p=1,2,\ldots$.

$C^{0\pi}_p$: $\Sigma(x_0,x_1)=\Sigma(x_p,x_{p+1})=1/(2p)$, $\Sigma(x_i,x_{i+1})=1/p$ for $I=1,\ldots,p-1$, with the definition $\Sigma(x_j,\lambda_j)\equiv 1/(2p)$ for $j=1,\ldots,p-1$, where $p=1,2,\ldots$. Assume further that $\sigma(x)$ changes its sign at all of $x=x_i$, $i=1,\ldots,p$. In the case C_{p+1} the stationary solution on $x_i<x<x_{i+1}$ is given by $(p+1,\lambda_i)$ for all $i=0,1,\ldots,p$. In the case $C^0_{p+1/2}$ the solution on $x_0<x<x_1$ is $(p+\frac{1}{2},0)$ while on $x_i<x<x_{i+1}$ it is $(p+\frac{1}{2},\lambda_i)$ for $i=1,\ldots,p$. If $C^\pi_{p+1/2}$ is the case, the solution on $x_i<x<x_{i+1}$ is $(p+\frac{1}{2},\lambda_i)$ for $i=0,1,\ldots,p-1$, but on $x_p<x<x_{p+1}$ it is $(p+\frac{1}{2},\pi)$. Finally, if $C^{0\pi}_p$ is the case, the solution on $x_i<x<x_{i+1}$ is (p,λ_i) for $i=1,\ldots,p-1$ while on $x_0<x<x_1$ and $x_p<x<x_{p+1}$ they are $(p,0)$ and (p,π), respectively.

Proof. We note that Theorem (b) corresponds to the case C_{p+1} with $p=0$. Assume that a boundary layer is at $0<x^*<\pi$, and define

$$x\equiv x^*+\nu\xi,\quad V^*(\xi)\equiv V_\nu(x^*+\nu\xi)\ ,$$

$$E^*(\xi)\equiv E_\nu(x+\nu\xi),\quad K^*(\xi,t)\equiv K(x^*+\nu\xi,t)\ .$$

By the arguments given in Appendix B we have the general form

$$K^*(\xi,t)=k(t)\int^\xi d\eta\exp\left[\int_\eta^\xi V^*(\zeta)d\zeta\right]\ ,\qquad -\infty<\xi<\infty \tag{C1}$$

for the kernel in the boundary layer. The form of $K^*(\xi,t)$ is again separated in t and ξ; this fact implies (B6)—(B8). One point to be noted is that $K^*(-\infty,t)$ and $K^*(+\infty,t)$ must have different signs at all $t\geqq 0$. Therefore, $\sigma(x)$ must change its sign crossing $x=x^*$, which necessitates that x^* is a zero of $\sigma(x)$ with alternating signs on both sides. Another point is that the matching conditions give restrictions that $V^*(\pm\infty)$, $E^*(\pm\infty)$, and $K^*(\pm\infty,t)$ be finite. The solution of (B9) under $|\phi_\pm(\pm\infty)|<\infty$ has again the unique form $\phi_\pm(\xi)=-\kappa\tanh[\kappa(\xi-\xi_0)/2]$ with $\kappa\geqq 0$. This fact binds again the inviscid solution $V(x)$ obeying (B3) to be increasing within the range

$$-\gamma/2^{1/2}\leqq V(x)\leqq\gamma/2^{1/2}\ . \tag{C2}$$

Otherwise, $V(x)$ (assumed to be continuous in x until it meets a boundary layer) has a constant sign so that one of the ends of this segment of the inviscid solution cannot be matched to a boundary layer or cannot fulfill by itself the boundary condition. Let two consecutive boundary layers be located at $x_1<x_2$, with respective characteristic constants $\kappa_1\geqq\kappa_1'\geqq 0$ and $\kappa_2\geqq\kappa_2'\geqq 0$ of (B10). At $x=x_1+0$ we have for the inviscid solution with γ of (B1)

$$-\gamma/2^{1/2}\leqq-(\kappa_1+\kappa_1')=V(x_1+0)\leqq 0\ ,$$

$$(\kappa_1-\kappa_1')^2=E(x_1+0)\geqq\gamma^2/2\ .$$

Thus we have $\kappa_1=\gamma/2^{1/2}$ and $\kappa_1'=0$. The arguments proceed in the same manner at $x=x_2-0$ yielding $\kappa_2=\gamma/2^{1/2}$, $\kappa_2'=0$. These prove: All of the segments of inviscid solutions on $x\in X$ have one and the same $\gamma>0$, and all of the boundary layers have the same $\kappa=\gamma/2^{1/2}$ and $\kappa'=0$.

Suppose $0\leqq x_1<x_2<\ldots<x_n\leqq\pi$ be the locations of boundary layers which must all be zeros of $\sigma(x)$ with alternating signs. By $V(x_i\pm 0)=\mp\gamma/2^{1/2}$ and by (B4) there holds (cf. Fig. 11)

$$\Sigma(x_i,x_{i+1})=(2^{5/2}/3)\gamma^3 .$$

Taking into account the complications that $x=0$ or π may be either a boundary layer or a zero (the center of antisymmetry[13]) of the inviscid $V(x)$, we obtain the possible values of γ in (28) from (3), together with respective forms of stationary solutions stated in (c*). The replacement with long-time averages is justified by the same reasoning as in Appendix B.

---

[1]J. M. Burgers, Proc. R. Neth. Acad. Sci. **43**, 2 (1940); Adv. Appl. Mech. **1**, 171 (1948); *The Nonlinear Diffusion Equation* (Reidel, Dordrecht, 1974).

[2]The restriction on $\sigma(0)$ and $\sigma(\pi)$ in (2) avoids unnecessary complications that may arise in the limit $\nu\downarrow 0$ with, e.g.,

$$\partial^2 u_\nu/\partial x^2 \mid_{\partial X} = -\sigma(x) \mid_{\partial X} f(t)/\nu .$$

[3]H. Nakazawa, Prog. Theor. Phys. **64**, 1551 (1980).

[4]H. Nakazawa, Adv. Appl. Math. **3**, 18 (1982).

[5]H. Nakazawa, Prog. Theor. Phys. **65**, 1565 (1981).

[6]The following is a special consequence of the general entropy condition given by O. A. Oleinik, Usp. Mat. Nauk **12**, 3 (1957); Am. Math. Soc. Transl. (2), **26**, 95 (1963).

[7]H. Nakazawa, in the Proceedings of the First International Conference on the Physics of Phase Space [*Lecture Notes In Physics* (to be published)].

[8]H. Nakazawa (unpublished).

[9]This may be seen heuristically with (5), whose derivation is seen also below Eq. (B9) in Appendix B.

[10]A. Friedman, *Stochastic Differential Equations and Applications* (Academic, New York, 1975), Vol. I.

[11]If a portion of the profile attains $u'_\nu(Z(t),t)<0$, then the self-convection term $u_\nu u'_\nu$ drives its neighboring segments to form a shock front. Therefore, $u'_\nu(Z(t),t)=0$ is a necessary condition for the birth of a new zero with $u'_\nu(Z(t),t)>0$ that arises in pair with, and on the other side of, a shock front. Figure 3 may thus be interpreted as stipulating that the possibility for $u_\nu(Z,t)=u'_\nu(Z,t)=0$ occurs only near walls for $\sigma(x)\neq 0$ on $0<x<\pi$, which is natural.

[12]C. Bardos, in *Nonlinear Partial Differential Equations and Applications*, edited by J. M. Chadan, Vol. 648 of *Lecture Notes In Mathematics* (Springer, Berlin, 1978), cf. specifically p. 14.

[13]The problem (1) may be extended to $x\in R$ by using antisymmetric extensions at $x=n\pi$ with integer n. We say a point $x\in X$ is a center of antisymmetry if it is so in the extended problem on $x\in R$.

[14]Equation (23) is obtained by decomposing $u_\nu(x,t)$ in a series of Wick polynomial functionals of $\{f(t');s\leqq t'\leqq t\}$, and truncating at the first nontrivial level. The structure of this approximation is discussed in H. Nakazawa, Prog. Theor. Phys. **56**, 1411 (1976); **57**, 346 (1977), where the scheme was called Gaussian approximation.

[15]H. Ito, Prog. Theor. Phys. **66**, 337 (1981); J. Stat. Phys. **37**, 653 (1984).

[16]*Laminar Boundary Layers*, edited by L. Rosenhead (Oxford University Press, Oxford, 1963); G. K. Batchelor, *An Introduction to Fluid Dynamics* (Cambridge University Press, Cambridge, 1967).

[17]Any improved pure states [random fields for $v(x,t)$] a and c should give the average $\overline{V}_i(x)$ for $i=a$ or c that fulfill $\overline{V}_a(x)=-\overline{V}_c(\pi-x)$, $\overline{E}_a(x)=\overline{E}_c(\pi-x)$, $\overline{V}_{ac}(x)<V_b(x)$ on $\pi/2<x<\pi$ and $\overline{E}_{ac}(x)<E_b(x)$, where $\overline{V}_{ac}$ and $\overline{E}_{ac}$ refer to the even mixture of a and c. These states should further incorporate some kinematical features of (17)–(18), at least respecting the entropy condition at $x=0$ and π to some quantitative extent. The deterministic model in the text will be the simplest nontrivial example of these (improved?) pure states.

[18]P. D. Lax, Commun. Pure Appl. Math. **7**, 159 (1954).

[19]By the uniqueness of the stationary state, we took a feasible initial data that seems to prompt the convergence of time averages.

[20]Figure 3 of Ref. 7, which refers to the same numerical run as the present Fig. 8 in a normalization different from (3), is shown with ordinates of $W(t)$ and $P(t)$ for ± 3 but that of the energy for 4. This scaling was overlooked in Ref. 7; the first line below its Fig. 2 should read "... P shows peaks at $P=0$ and $P=\pm 0.6\sim\mp 1.8$ which ... ."

[21]The run for $0\leqq t\leqq 73.74$ ($=201\,920\Delta t$) takes 6.5 minutes of central-processing unit (CPU) time on the *FACOM-M382/M380* system of Kyoto University.

[22]This is another point which was malanticipated to be always long in Ref. 8.

[23]If $q(x)$ is absolutely continuous on $x\in X$, then its total variation on X is $||q(x)||_{\mathrm{BV}}=\int_X \mid q'(x) \mid dx$.

[24]In this sense the forced Burgers fluid in the inviscid limit substantiates, verbally, the subjectivity of turbulence phenomena and their organized structures stressed recently by A. Hasegawa, Adv. Phys. **34**, 1 (1985), on the basis of (inverse) cascade mechanisms considered to be installed in various fluids and plasmas. However, no Kolmogorov-type spectrum shows up on (1), and its energy never cascades to wave numbers smaller than n for $\sigma(x)\propto\sin(nx)$ with $n>2$, as described in Sec. V. The basic mechanism for the quasistationary structures on (1) is different from cascade processes, and still awaits for physical interpretations.